Cancer Gene Therapy (2002) 9, 296–307

www.nature.com/cgt

Effectiveness of insulin-like growth factor I receptor antisense strategy against Ewing's sarcoma cells

Katia Scotlandi,[1] Cecilia Maini,[1] Maria Cristina Manara,[1] Stefania Benini,[1] Massimo Serra,[1] Vanessa Cerisano,[1] Rosaria Strammiello,[1] Nicola Baldini,[1] Pier-Luigi Lollini,[2] Patrizia Nanni,[2] Giordano Nicoletti,[3] and Piero Picci[1]

[1]Laboratorio di Ricerca Oncologica, Istituti Ortopedici Rizzoli, Bologna, Italy; [2]Istituto di Cancerologia, Università degli Studi di Bologna, Bologna, Italy; and [3]Istituto Nazionale per la Ricerca sul Cancro-Genova, Sezione di Biotecnologie di Bologna, Bologna, Italy.

The insulin-like growth factor I receptor (IGF-IR) plays an essential role in the establishment and maintenance of transformed phenotype of Ewing's sarcoma (ES) cells, and interference with the IGF-IR pathways by a neutralizing antibody causes reversal of the malignant potential of this neoplasm. In this paper, we stably transfected an IGF-IR antisense mRNA expression plasmid in an ES cell line to determine the effectiveness of antisense strategies against the *in vitro* and *in vivo* growth of ES cells. Doxorubicin sensitivity of TC-71 cells expressing antisense targeted to IGF-IR mRNA was also examined. Cells carrying antisense IGF-IR had a reduced expression of the receptor, a modest decrease in cell proliferation, a significant increase in anoikis-induced apoptosis, and a severely reduced ability to form colonies in soft agar. Moreover, TC/AS cells showed a marked reduction in their motility. *In vivo*, when cells carrying antisense IGF-IR were injected subcutaneously in nude mice, tumor formation was delayed and survival increased. Metastatic ability of ES cells was also significantly reduced. Furthermore, TC/AS clones showed a significantly higher sensitivity to doxorubicin — a major drug in the treatment of ES. These results indicate that inhibiting IGF-IR by antisense strategies may be relevant to the clinical treatment of ES patients by reducing the malignant potential of these cells and enhancing the effectiveness of chemotherapy.

Cancer Gene Therapy (2002) **9,** 296 – 307 DOI: 10.1038/sj/cgt/7700442

Keywords: Ewing's sarcoma; insulin-like growth factor I; antisense; malignancy; nude mice

Ewing's sarcoma (ES) is a malignant small round cell tumor of bone and soft tissues, preferentially arising in children and young adults. ES is characterized by the presence of specific chromosomal translocations, which produce *EWS/ets* gene rearrangements [in more than 95% of cases, the gene fusion is EWS/FLI-1 due to the t(11;22)(q24;q12), or EWS/ERG due to the t(21;22)(q22;q12)],[1] as well as the expression, at extremely high levels, of an antigen encoded by the *MIC2* gene (also known as CD99 or p30/32^{MIC2}).[2,3] ES shows an extremely aggressive clinical course. At diagnosis, approximately 25% of patients has detectable metastases in the lungs and/or bones and bone marrow, but nearly all patients have micrometastases, as evidenced by a less than 10% cure rate with local therapy alone.[4] The adoption of multimodal treatments with very aggressive chemotherapeutic regimens associated with surgery or radiotherapy for local control has significantly improved the chance of survival of ES nonmetastatic patients, shifting the 5-year survival rate to around 50–60%.[5,6] However, despite advances in therapy, one third of patients with nonmetastatic disease, and the great majority of patients with metastases at diagnosis, do not survive, regardless of therapy.[7] Furthermore, recent clinical studies have indicated that the survival rate of ES patients has reached a plateau phase and, possibly, the highest levels achievable by conventional multimodal therapy.[8,9] Successful treatment of therapy-resistant disease therefore requires new strategies.

Recent findings have indicated the insulin-like growth factor I receptor I (IGF-IR) as a promising target for tailored biological therapies of ES. IGF-IR is implicated in the autocrine and paracrine control of ES growth and appears to be particularly important in the pathogenesis of this tumor. In particular, IGF-IR–mediated loop is constantly present in ES and is a major autocrine circuit of this neoplasm.[10,11] In addition, Toretsky et al[12] reported IGF-IR expression to be necessary for EWS/FLI-1–mediated transformation of primary fibroblasts. Thus, the IGF-IR pathway may be considered a good site for therapeutic intervention in EWS-FLI-1–mediated tumor proliferation. We confirmed this finding by demonstrating that impairment of IGF-IR by neutralizing antibody and suramin reduces growth and increases apoptosis of ES cells both *in vitro* and *in vivo*, and significantly decreases migration, invasion, and metastatic spread to the lungs and

Received December 13, 2001.

Address correspondence and reprint requests to: Dr Katia Scotlandi, Laboratorio di Ricerca Oncologica, Istituti Ortopedici Rizzoli, Via di Barbiano, 1/10, Bologna 40136, Italy. E-mail: katia.scotlandi@ior.it

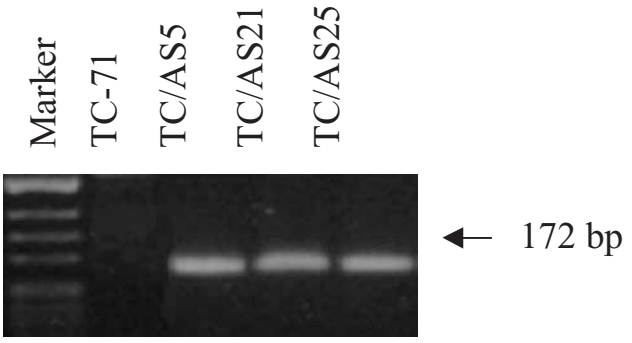

Figure 1 PCR analysis of TC-71–transfected clones for the presence of a plasmid expressing antisense RNA to the IGF-IR. The expected PCR product size is 172 bp; because the amplimers are in different exons separated by a large intron, only plasmid DNA is detected by this method. PCR was performed with a 55°C annealing temperature for 40 amplification cycles.

bones.[13] In this study, we explored the preclinical effectiveness of antisense IGF-IR therapy both in terms of inhibition of the *in vitro* and *in vivo* growth of ES cells and by increasing their sensitivity to conventional chemotherapeutic agents.

Materials and methods

Cell line and transfection

ES cell line TC-71 was a generous gift from TJ Triche (Children Hospital, Los Angeles, CA). Cells were routinely cultured in Iscove modified Dulbecco's medium (IMDM), supplemented with 100 U/mL penicillin, 100 μg/mL streptomycin (Life Technologies, Paisley, Scotland, UK), and 10% inactivated fetal calf serum (FCS) (Biological Industries, Kibbutz Beth Haemek, Israel). TC-71 cells were maintained in a humidified 5% CO_2 atmosphere. We also used cell lines derived from TC-71, expressing an antisense or a sense mRNA to the IGF-IR mRNA. These cell lines were obtained by a calcium phosphate transfection with a plasmid (HSPIGF-IR; kindly gifted from R Baserga, Kimmel Cancer Center, Thomas Jefferson University, Philadelphia, PA) that contains a 309-bp fragment of a human IGF-IR cDNA in either the sense or antisense direction, under the control of the *Drosophila* HSP70 promoter. These cells were cultured in IMDM plus 10% FCS plus 500 μg/mL G418 (Sigma, St. Louis, MO) to maintain stable transfectants.

Polymerase chain reaction (PCR)

PCR was performed to verify the presence of the plasmid in the transfectants. Genomic DNA was extracted by DNAzol extraction kit (Life Technologies), according to the manufacturer's instructions. DNA (500 ng) was amplified by PCR using the amplimers previously reported.[14] The expected PCR product size is 172 bp; because the amplimers are in different exons separated by a large intron, only plasmid DNA is detected by this method. PCR was performed with a 55°C annealing temperature for 40 amplification cycles.

Quantitative real-time RT-PCR

Total RNA was extracted by TRIzol extraction kit (Life Technologies) from IGF-IR sense and antisense transfectants maintained at 35°C (controls) and 39.6°C, a temperature reported to induce the expression of sense and antisense transcripts,[14,15] for 72 hours. The quality of the RNA samples was determined by electrophoresis through agarose gels and staining with ethidium bromide, and the 18*S* and 28*S* RNA bands were visualized under UV light. Real-time fluorescence detection method[16,17] was used to analyze the relative level of IGF-IR expression in our transfectants. In particular, 1 μg of total RNA was denatured at 65°C for 10 minutes and then reverse-transcribed in a 100-μL reaction mixture containing 500 μM of each dNTP, 125 U of MultiScribe Reverse Transcriptase (Applied Biosystems, Foster City, CA), 40 U of RNase Inhibitor (Applied Biosystems), 2.5 μM oligo $d(T)_{16}$, 1× TaqMan RT Buffer, 5 mM $MgCl_2$ at 48°C for 40 minutes. Reactions omitting enzyme or RNA were used as negative controls. TaqMan primers and probes for the quantitative detection of human glyceraldehyde-3-phosphate dehydrogenase (GAPDH) and IGF-IR were designed by using Primer Express software (Applied Biosystems) to work in the same cycling conditions (95°C for 10 minutes followed by 40 cycles at 95°C for 15 seconds and 60°C for 1 minute) generating products with sizes of 224 and 70 bp, respectively. PCR primer and probe sequences were as follows (all 5′ to 3′ direction): *IGFIR*: forward GAA AGT GAC GTC CTG CAT TTC A, reverse CCG GTG CCA GGT TAT GAT G, probe: FAM-TCC ACC ACC ACG TCG AAG AAT CGC; *GAPDH*: forward GAA GGT GAA GGT CGG AGT C, reverse GAA GAT GGT GAT GGG ATT TC, probe: FAM-GAA GCT TCC CGT TCT CAG CC.

All PCR reactions were performed by using a ABI PRISM 7700 Sequence Detection System (Applied Biosystems). Standard curves for both target and reference gene were made by using 5-fold serial dilutions of TC-71 cDNA. All samples were run in triplicate. Reactions are characterized by the point during cycling when amplification of the PCR product is first detected, rather than the amount of PCR product accumulated after a fixed number of cycles. The larger the starting quantity of the target molecule, the earlier a significant increase in fluorescence is observed. The parameter C_T (threshold cycle) is defined as the fractional cycle number at which the fluorescence generated by cleavage of the probe passes a fixed threshold above baseline. The IGF-IR mRNA is quantified by measuring C_T to determine the relative expression. In all the experiments, the threshold value used to determine C_T during analysis was kept constant. Data were normalized to GAPDH. The relative IGF-IR mRNA expression was also normalized to a calibrator, consisting of the parental TC-71 mRNA, and calculated by using the formula: $2^{-\Delta\Delta CT}$ where $\Delta CT = C_T$ IGF-IR $- C_T$ GAPDH and $\Delta\Delta C_T = \Delta C$t sample $- \Delta C$T calibrator.

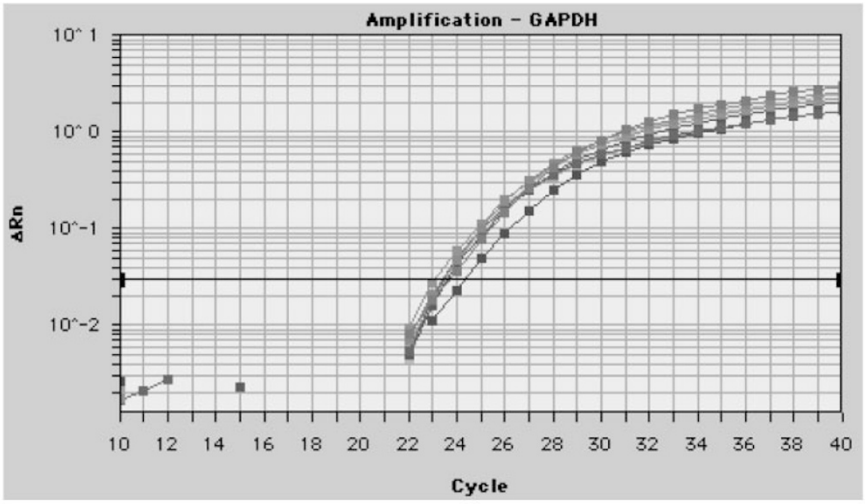
Amplification - GAPDH
10^ 1
10^ 0
10^-1
10^-2
ΔRn
10 12 14 16 18 20 22 24 26 28 30 32 34 36 38 40
Cycle

A

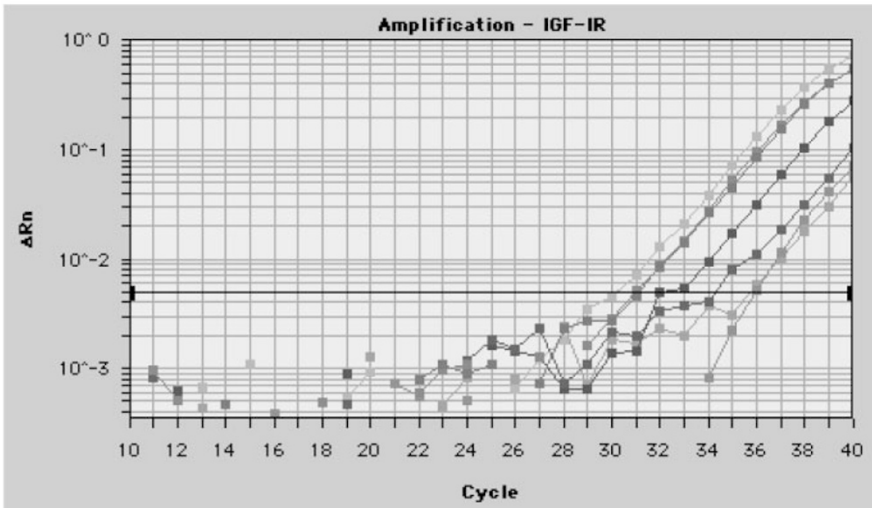
Amplification - IGF-IR
10^ 0
10^-1
10^-2
10^-3
ΔRn
10 12 14 16 18 20 22 24 26 28 30 32 34 36 38 40
Cycle

B

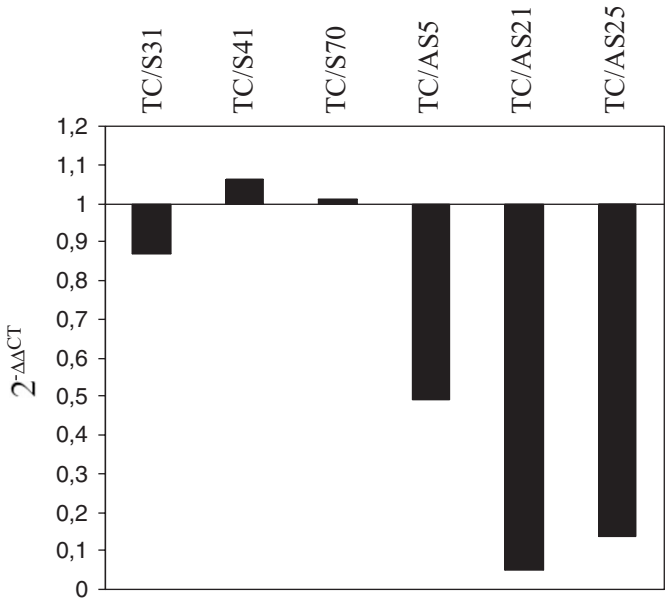
TC/S31
TC/S41
TC/S70
TC/AS5
TC/AS21
TC/AS25
1,2
1,1
1
0,9
0,8
0,7
0,6
0,5
0,4
0,3
0,2
0,1
0
$2^{-\Delta\Delta CT}$

C

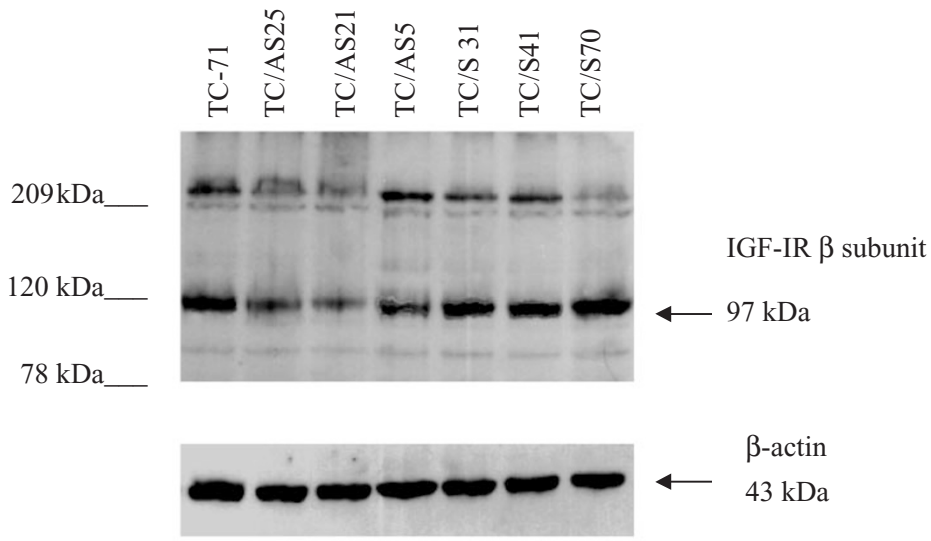

Figure 3 Western blot analysis of IGF-IR expression levels in TC-71–derived clones. Cell lysates, collected after 72 hours at 39.6°C, were stained with an antibody to the β-subunit of the IGF-IR. In the lower panel, the same blot was stripped and reprobed with the mAb for actin protein.

All samples were resolved in a 2% agarose gel to confirm the PCR specificity.

Western blot

Proteins were extracted from different cell lines maintained at 35°C (controls) and 39.6°C for 72 hours by using NP40 1% lysis buffer [10 mM Tris–HCl (pH 7.4), 150 nM NaCl, 50 mM EDTA, IGEPAL 1%, 1 mM PMSF, 10 μg/mL Aprotinin, 0.2 mM Na_3VO_4] and sonication. The concentration of total protein was measured using the Bio-Rad (Munich, Germany) protein assay, according to the method of Bradford.[18] Equal amounts of protein (60 μg) were analyzed by sodium dodecyl sulfate polyacrylamide gel electrophoresis with an 8% separation gel at 130 V for 60 minutes and transferred at 42 V for 90 minutes to nitrocellulose sheets. Blots were incubated with anti–hIGF-IR-β antibody (Santa Cruz Biotechnology, Santa Cruz, CA; 1/1000 dilution), and then with the horseradish peroxidase–linked secondary antibody (Dako, Glostrup, Denmark; 1/1500 dilution), revealed by ECL Western blotting detection reagents (Amersham, Aylesbury, UK). The same blot was stripped and reprobed with the monoclonal antibody for actin protein (Chemicon International, Temecula, CA; diluted 1: 1000).

In vitro *growth*

To study the effects of IGF-IR down-regulation, 20,000 cells/cm^2 were seeded in IMDM plus 10% FCS and incubated at 35 and 39.6°C. After 24 hours, medium was changed with IMDM plus 1% FCS, or IMDM plus 1% FCS with IGF-I (50 ng/mL; United Biomedical, Lake Placid, NY). Cell growth was evaluated on harvested cells by trypan blue vital cell count.

Poly-2-hydroxyethylmethacrylate (poly-HEMA) assay

Six-well plates were treated with poly-HEMA (Sigma) following the Folkman and Moscona method.[19] Briefly, wells were treated with a 1-mL solution of poly-HEMA diluted in ethanol 95% (12 mg/mL) and left to dry at room temperature. Before use, poly-HEMA–coated dishes were washed twice in phosphate-buffered solution (PBS) and once in Hank's solution. Seeded were 100,000 cells/well in IMDM 1% FCS and incubated at 39.6°C in a humidified 5% CO_2 atmosphere. Viable and dead cells were counted after 24, 48, and 72 hours. Detection and quantification of apoptotic cells were also obtained by Mountain View, CA flow cytometric analysis (FACSCalibur; Becton Dickinson) of annexin V–labelled cells performed according to the manufacturer's instructions (Roche Diagnostic, Mannheim, Germany). Briefly, 1×10^6 cells were washed with PBS and incubated with 100 μL of the following solution: 20 μL of annexin V–FITC, 20 μL of propidium iodide (PI), and 1 mL of HEPES buffer. PI incorporation was evaluated in association with the fluorescent signal intensity to allow the discrimination of necrotic and apoptotic cells.

Figure 2 Relative expression of IGF-IR mRNA in TC-71 clones transfected with a plasmid expressing sense (TC/S) or antisense (TC/AS) RNA to the IGF-IR by real-time PCR. Representative real-time amplification plots of GAPDH **(A)** and IGF-IR **(B)** for the TC-71 cell line (green squares) and derived clones (TC/S31, dark green squares; TC/S41, yellow squares; TC/S70, red squares; TC/AS5, dark blue squares; TC/AS21, blue squares; TC/AS25, pink squares) were shown. Triplicate for each sample was performed, but the data for only one is shown here. RNA was extracted from cells maintained at 39.6°C for 72 hours. **C:** The relative IGF-IR mRNA expression of TC-71–transfected clones with respect to the parental cell line used as calibrator ($2^{-\Delta\Delta CT}=1$). Mean values of the triplicate samples were used for calculations.

Soft agar assay

Anchorage-independent growth was determined in 0.33% agarose (SeaPlaque; FMC BioProducts, Rockland, ME) with a 0.5% agarose underlay. One thousand and 3,300 cells were plated in semisolid medium (IMDM 10% FCS plus agar 0.33%) and incubated at 39.6°C in a humidified 5% CO_2 atmosphere. Colonies were counted after 6 days.

Motility assay

TC-71 cells and derivates were maintained at 39.6°C in IMDM 10% FCS for 72 hours. Motility assay was

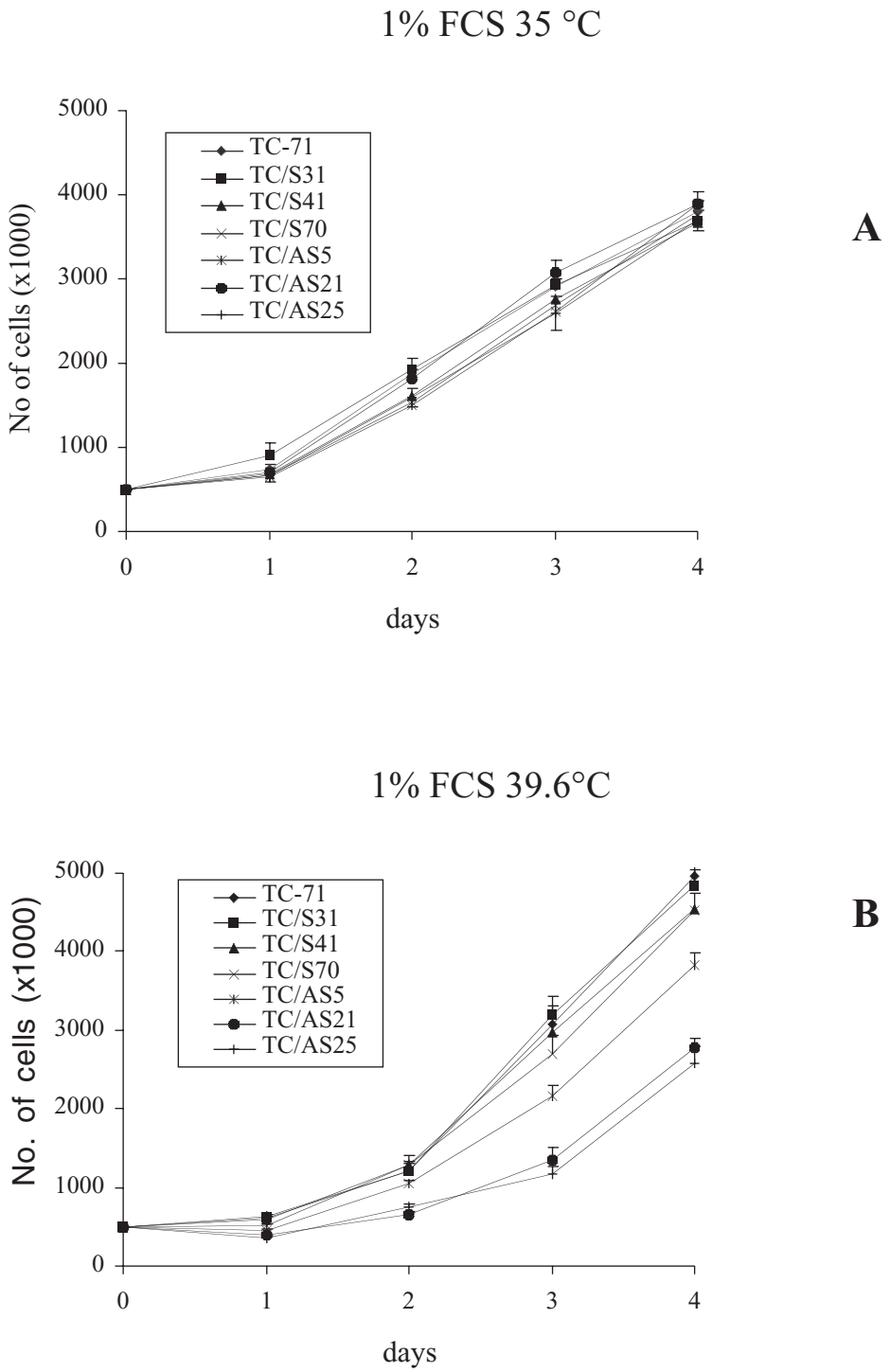

Figure 4 *In vitro* growth curves of TC-71 cells and derived clones at 35°C **(A)** and 39.6°C **(B)**. Cells were seeded in IMDM 10% FCS. After 24 hours, medium was replaced with IMDM 1% FCS and the number of cells was estimated at the indicated times (*abscissa*). Results represent the mean ± SE of duplicate experiments. TC/S, sense-transfected clones; TC/AS, antisense-transfected clones.

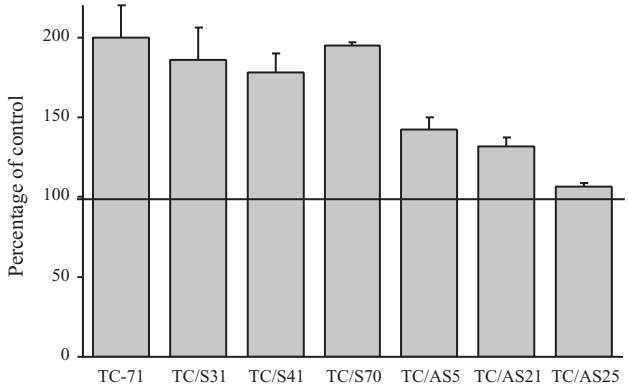

Figure 5 IGF-I dependence of TC-71 cells and derived clones in monolayer growth at 39.6°C. Cells were seeded in IMDM 10% FCS. After 24 hours, medium was replaced with IMDM 1% FCS with or without (controls) IGF-I (50 ng/mL). The cell number was counted after 72 hours of incubation and is expressed as percentage of corresponding controls. Results represent the mean ± SE of duplicate experiments. TC/S, sense-transfected clones; TC/AS, antisense-transfected clones.

performed using Transwell chambers (Costar, Cambridge, MA) with 8-μm pore size, polyvinylpyrrolidone-free, polycarbonate filters (Nucleopore, Pleasanton, CA). IMDM plus 10% FCS alone or IMDM plus 10% FCS with IGF-I (50 ng/mL) (United Biomedical) were placed in the lower compartment of the chamber. 10^5 cells in IMDM plus 10% FCS were then seeded in the upper compartment and incubated for 18 hours at 39.6°C. Cells migrated towards the filter to reach the lower chamber base and were counted after Giemsa staining. All of the experiments were made in triplicate.

In vitro *sensitivity to doxorubicin (DXR)*

20,000 cells/cm^2 were seeded in IMDM 10% FCS and incubated at 39.6°C in a humidified 5% CO_2 atmosphere. After 24 hours, medium was changed with IMDM 10% FCS containing different concentrations of DXR (100 pg/mL–100 ng/mL) (Sigma). Cells were harvested and counted after 72 hours of treatment to estimate the percentage of growth inhibition compared to the appropriate controls. Moreover, anchorage-independent growth of IGF-IR sense and antisense transfectants was also analyzed after exposure to DXR. Briefly, cells were exposed to different concentrations of DXR for 16 hours — a time corresponding to the doubling time of these cells — seeded in semisolid medium following the same procedures that were described above, and colonies were counted after 6 days.

Tumorigenic and metastatic ability in athymic mice

Female athymic 4- to 5-week-old Crl:nu/nu (CD-1) BR mice (Charles River Italia, Como, Italy) were used. Tumorigenicity was determined after subcutaneous (s.c.) injection of 5×10^6 cells. Tumor growth was assessed once a week by measuring tumor volume, calculated as $\pi/6[\sqrt{(ab)}]^3$, where a and b are the two major diameters. For ethical reasons, mice were sacrificed and necropsied when the mean tumor volume was 5 mL. Tumors were fixed in 10% buffered formaldehyde for at least 48 hours and processed for histological examination. Tumor sections were stained with hematoxylin and eosin, and analyzed microscopically. The metastatic ability was determined by injection of 2.5×10^6 viable cells in a tail lateral vein. Two months later, mice were sacrificed. The number of experimental pulmonary metastases was determined by counting with a stereomicroscope after staining with black India ink. The experimental procedures were approved by the local ethical committee and were performed according to the latest version of the Declaration of Helsinki.

Statistical analysis

Differences among means were analyzed using Student's *t* test. Wilcoxon's rank sum test and Fisher's exact test were used for frequency data. Kaplan-Meier plots and log-rank test were used to evaluate the survival of mice injected with

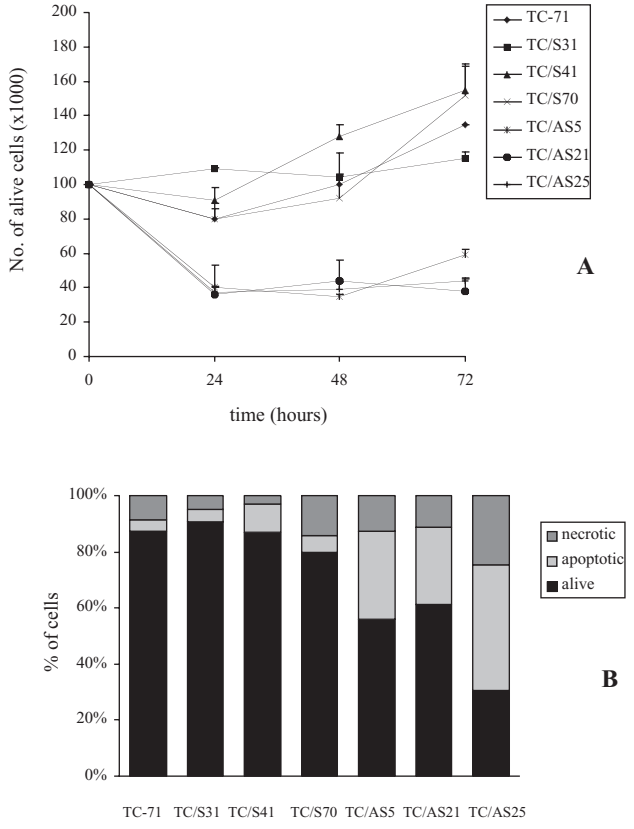

Figure 6 Survival of TC-71 cells and derived clones on poly-HEMA–coated dishes. 10^5 cells were seeded on poly-HEMA–coated dishes in IMDM 1% FCS at 39.6°C. **A:** The number of alive cells per plate was determined by trypan blue vital cell count at the times indicated on the *abscissa*. Results represent the mean ± SE of triplicate experiments. **B:** Cytofluorometric analysis of apoptotic TC-71 cells and derivates by annexin V and PI after 24 hours. The simultaneous application of PI as a DNA stain, which is used for dye exclusion tests, allows the discrimination of necrotic cells from the annexin V positively stained cells. Results represent the mean of triplicate experiments. TC/S, sense-transfected clones; TC/AS, antisense-transfected clones.

Table 1 Growth in soft agar of TC-71 cells and derivates at 39.6°C

Cells	Number of colonies*	Percent inhibition	*P*†
TC-71	1734±144		
TC/S31	1723±206	1	
TC/S41	1519±393	12	
TC/S70	2010±61		
TC/AS5	908±35	48	.001
TC/AS21	584±159	66	.001
TC/AS25	680±132	61	.002

*Cells were seeded at a concentration of 3300 cells and the number of colonies in duplicate plates was determined after 6 days of growth in 10% FCS at 39.6°C. Data are expressed as means of four to six plates ±SE.

†Student's *t* test, with respect to TC-71 parental cells.

TC-71 cells. The analysis of drug combination effects was performed by using the fractional product method.

Results

Characterization of IGF-IR antisense (AS)-transfected clones

ES tumor cells were transfected with a vector where IGF-IR cDNA was expressed in the antisense or sense orientations under the control of a *Drosophila* HSP70 promoter. Among the several IGF-IR antisense clones (AS) obtained, three were selected and studied in comparison with parental TC-71 cells and IGF-IR sense control transfectant cells (S). The presence of antisense plasmid in genomic DNA of AS transfectants was demonstrated by PCR (Fig 1). The expression of IGF-IR appeared to be reduced in TC/AS transfectants in comparison with parental cells and TC/S clones, both at mRNA and protein level, as shown by real-time PCR (Fig 2) and Western blotting (Fig 3). Approximately 30–65% down-regulation of IGF-IR expression, normalized to the expression of actin, was observed by Western blotting in TC/AS clones.

In vitro *growth features of TC-71 cells expressing antisense RNA to IGF-IR*

The proliferation ability of TC/AS transfectants was comparable to that of parental and TC/S cells at 35°C, whereas it was impaired at 39.6°C (Fig 4, A and B) when cells were maintained in low serum medium. No significant differences were observed in the growth rate when cells were maintained in 10% FCS-containing medium (data not shown). TC/AS clones showed a lower growth dependence on exogenous IGF-I (Fig 5).

To analyze the effects of IGF-IR impairment on ES cell survival, independently of mitogenesis, we evaluated survival and apoptotic rate of TC/AS transfectants in poly-HEMA–coated dishes — a method originally proposed by Folkman and Moscona[19] that was reported to induce anoikis (apoptotic death of cells prevented to adhere to extracellular matrix).[20,21] Under these conditions, the survival of TC/AS transfectants was severely reduced (Fig 6A) and the occurrence of apoptosis was significantly higher, as documented by annexin test (Fig 6B). When cells were prevented to adhere, IGF-IR impairment was more critical for anchorage-independent growth, i.e., colony

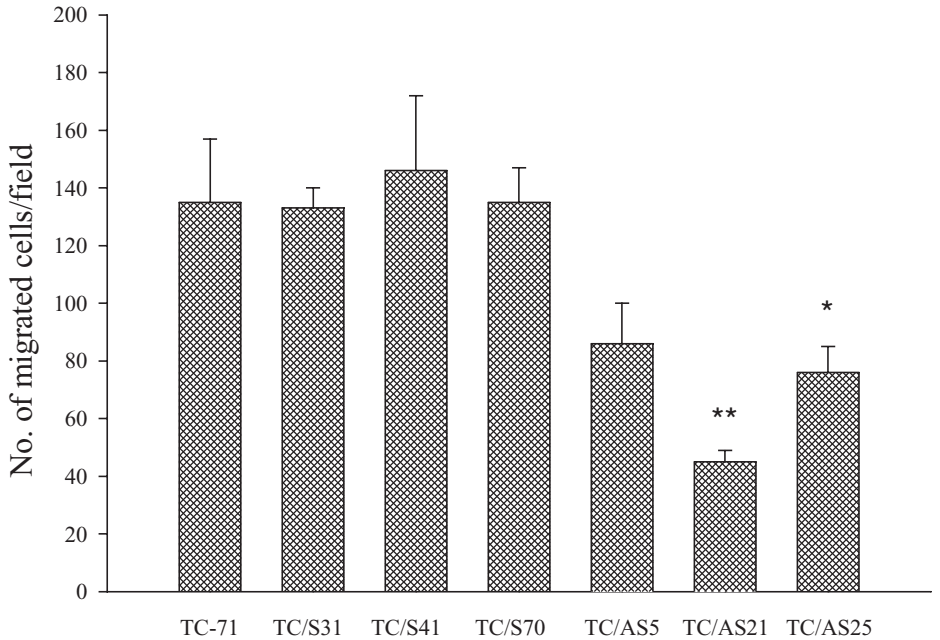

Figure 7 Migration ability of TC-71 cells and derived clones. Cells were preincubated at 39.6°C in IMDM 10% FCS for 72 hours, and then seeded in the upper compartment of a Transwell chamber. In the lower compartment, IMDM 10% FCS was used as the source of chemoattractant. Each column represents the mean of three independent experiments (*P=.01; **P<.001, Student's *t* test). TC/S, sense-transfected clones; TC/AS, antisense-transfected clones.

formation in soft agar, which is an accepted criterion for transformation,[22] than for growth in monolayer conditions. Cells expressing antisense to IGF-IR mRNA showed a significant inhibition of colony formation in soft agar compared to parental cells and cells expressing sense RNA (Table 1).

Moreover, antisense strategies against IGF-IR significantly affected the migratory ability of TC-71 cells. In fact, TC/AS transfectants showed a remarkably reduced mitogenicity, both when complete medium alone was used as a chemoattractant (Fig 7) and when IGF-I was added (data not shown).

In vivo *growth of TC-71 cells expressing antisense RNA to IGF-IR*

Tumorigenicity of TC-71 cells stably transfected with sense or antisense plasmids was examined after s.c. injection of parental cells and TC/S and TC/AS transfectants in athymic mice. All animals developed local tumors. However, in animals injected with TC/AS cells, tumor appearance was delayed (latency time: 13±1 and 17±2 days for TC-71 and TC/S31 cells; 22±4 and 28±5 days for TC/AS25 and TC/AS21, respectively; $P<.01$ with respect to parental cells) and tumor growth was slowed down (Fig 8). Four of five nude mice injected with TC/AS21 and one of five mice injected with TC/AS25 showed a remarkably lower growth rate with respect to controls. Survival was prolonged as well (Fig 9). To test the effect of IGF-IR impairment on the metastatic ability of ES cells, athymic mice were inoculated intravenously (i.v.) *via* the tail vein with 2.5×10^6 tumor cells. ES shows a high tendency to an early metastatic spread with a specific pattern of tissue distribution to lungs and/or bone. We have previously shown that TC-71 cells preferentially colonize to the skeleton after i.v. inoculation.[23] TC/AS transfectants showed a reduced metastatic ability. In fact, the incidence of metastases was reduced, both to the lungs (22% in animals injected with parental cells *vs* 0% in mice injected with TC/AS clones) and the skeleton (Fig 10). Furthermore, the time of appearance of extrapulmonary metastases was significantly delayed (44±2 and 46±3 days for TC-71 and TC/S31 cells *vs* 60±3 and 62 days for TC/AS25 and TC/AS21, respectively; $P<.01$, Student's *t* test). Similarly to tumorigenicity, TC/AS21

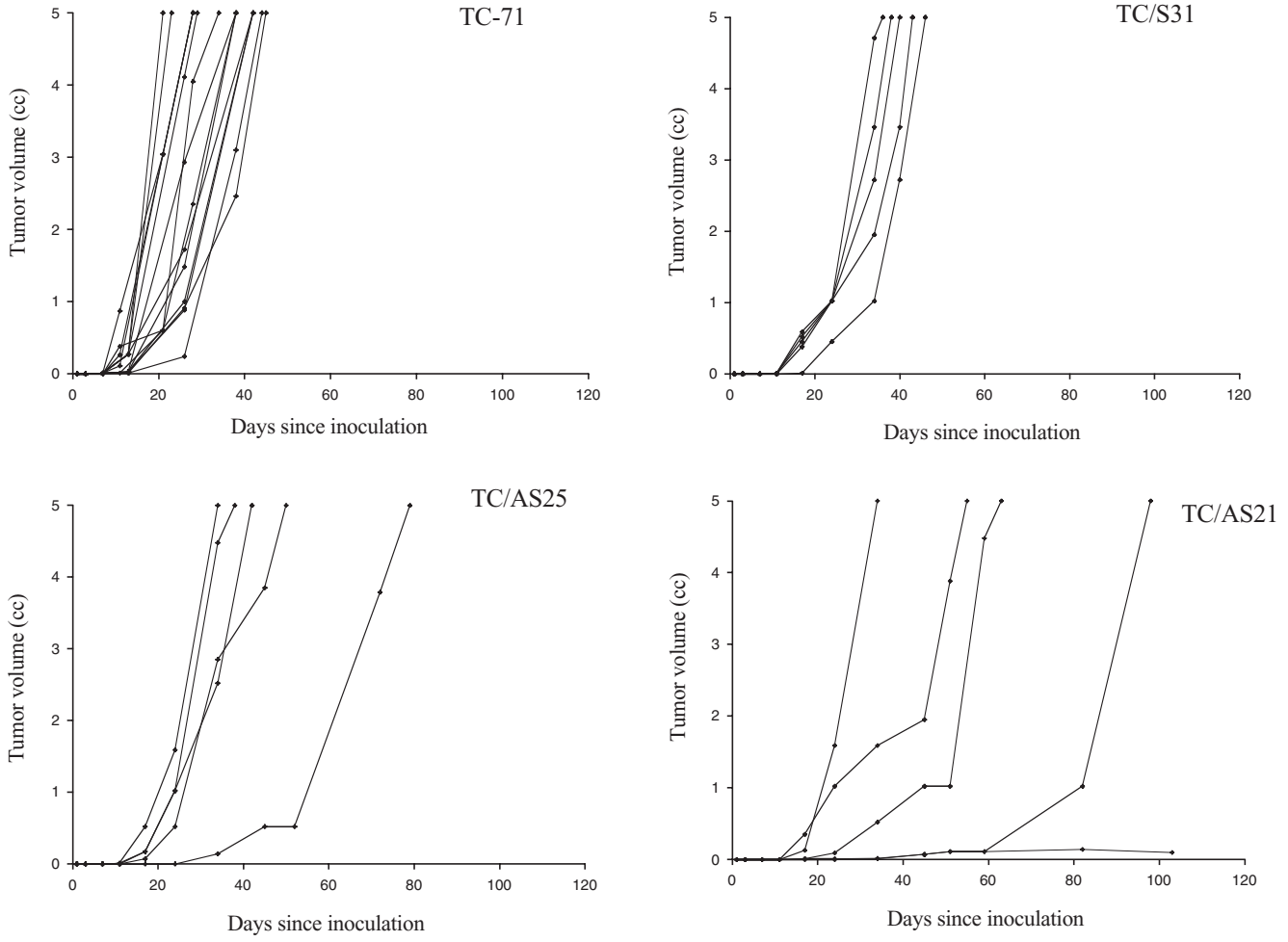

Figure 8 *In vivo* growth of two representative antisense-transfected clones as well as one sense clone and parental TC-71 cells injected s.c. in athymic mice. Each *line* corresponds to a single animal. TC/S, sense-transfected clones; TC/AS, antisense-transfected clones.

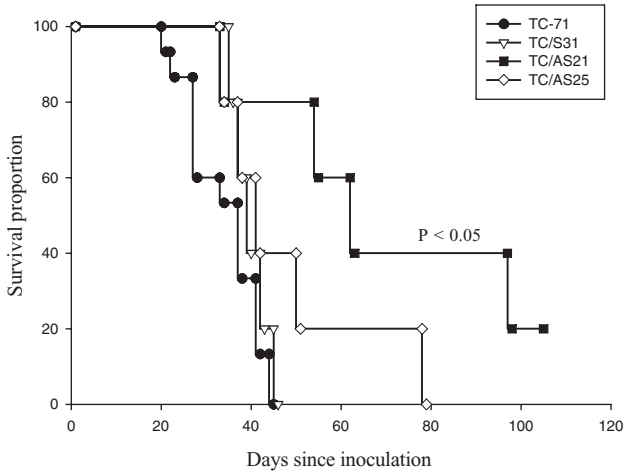

Figure 9 Survival of athymic mice s.c. injected with TC-71 and transfected cells. For ethical reasons, mice were sacrificed when the mean tumor volume was 5 mL. TC/S, sense-transfected clones; TC/AS, antisense-transfected clones. The animals injected with TC/AS21 cells survived significantly longer than mice injected with controls. Statistical significance was evaluated by the log-rank test.

transfectant showed the strongest inhibition in the metastatic potential.

Effects of IGF-IR antisense on ES chemosensitivity

The sensitivity of TC/AS clones to DXR, a key drug in the treatment of ES, was enhanced both in monolayer and in soft agar conditions. Figure 11 shows the significantly higher sensitivity of TC/AS transfectants to different doses of DXR compared to controls in conventional cytotoxic tests (A) and in soft agar clonogenic assays (B) ($P<.05$, Student's t test).

Discussion

ES cells provide a good model for the study of IGF-I regulation and effectiveness of strategies aimed at IGF-IR impairment. These cells secrete IGF-I and express IGF-IR,[10,11,24] which may account for autonomous cell growth, while maintaining a slight responsiveness to exogenous IGF-I.[13] Furthermore, of several autocrine circuits analyzed, only the IGF-IR–mediated loop is constantly present both in cell lines and clinical samples,[11] suggesting a role for this autocrine circuit in the pathogenesis of ES. Accordingly, Toretsky et al[12] have reported that IGF-IR expression is necessary for the transformation of primary fibroblasts by EWS-FLI-1, the genetic hallmark of ES cells. Consistent with these studies, a recent paper has shown that the most common type of EWS/FLI-1 fusion transcript, type 1, which is linked to a more favorable prognosis,[25] is also significantly associated with a lower proliferation rate of ES cells, possibly mediated by the differential regulation of IGF-IR pathways.[26] The importance of IGF-IR in modulating the malignant potential of ES cells has been further confirmed by the demonstration that an IGF-IR blocking antibody can reduce the growth and increase apoptosis both *in vitro* and *in vivo*, resulting in a significant inhibition of clonogenicity in soft agar, tumorigenicity and metastatic ability.[11,13] The migration ability of ES cells is also significantly reduced following IGF-IR impairment.[11] Finally, IGF-IR has been recently shown to protect ES cells from drug-induced apoptosis through PI 3-K and Akt survival signaling pathway.[27] In this paper, we evaluated the effectiveness of IGF-IR antisense strategies both *in vitro* and *in vivo* by transfecting TC-71 ES cells. This cell line, besides forming tumors in nude mice, is also a good experimental model for bone and lung metastases[23] because it mimics the pattern of metastatic ES involvement in humans.

Transfection with antisense sequences for growth factor receptors is effective in decreasing receptor expression and cell proliferation of neoplastic cells. Several models have been reported for IGF-IR in different neoplasms,[14,15,28–32] but no data were insofar reported on ES cells.

Antisense IGF-IR transfection produced clones with a moderately decreased IGF-IR expression, rather than fully negative phenotypes. The decrease in IGF-IR level obtained, however, was sufficient to determine an inhibition of the growth rate and a marked enhancement of apoptosis *in vitro*. In agreement with previous results,[14,15,31,32] which showed that IGF-IR has a more profound influence on the transformed phenotype than on cellular proliferation, we also found that the antisense strategy was more effective in inhibiting growth of TC-71 ES cells in soft agar than in monolayer conditions. In addition, the survival of TC/AS clones was severely impaired when cells were prevented to adhere to an extracellular matrix, and a significant increase in apoptosis due to anoikis was also observed, further

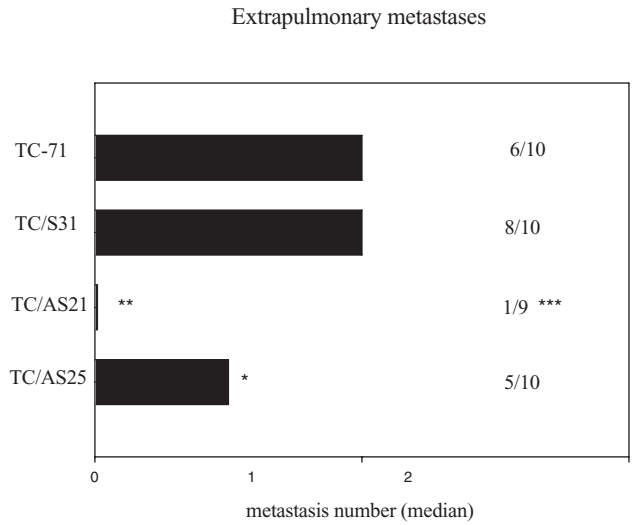

Figure 10 Metastatic ability to extrapulmonary sites of TC-71 and transfected cells. 2.5×10^6 cells were injected i.v. and metastases were evaluated 2 months after cell injection. Bars represent the median number of metastases; figure reports the number of mice with metastases/total number of mice. TC/S, sense-transfected clones; TC/AS, antisense-transfected clones. Significance: *$P<.05$, Wilcoxon's rank sum test with respect to TC/S31; **$P<.05$, Wilcoxon's rank sum test with respect to TC-71 or TC/S31; ***$P<.05$, Fisher's test with respect to TC-71 or TC/S31.

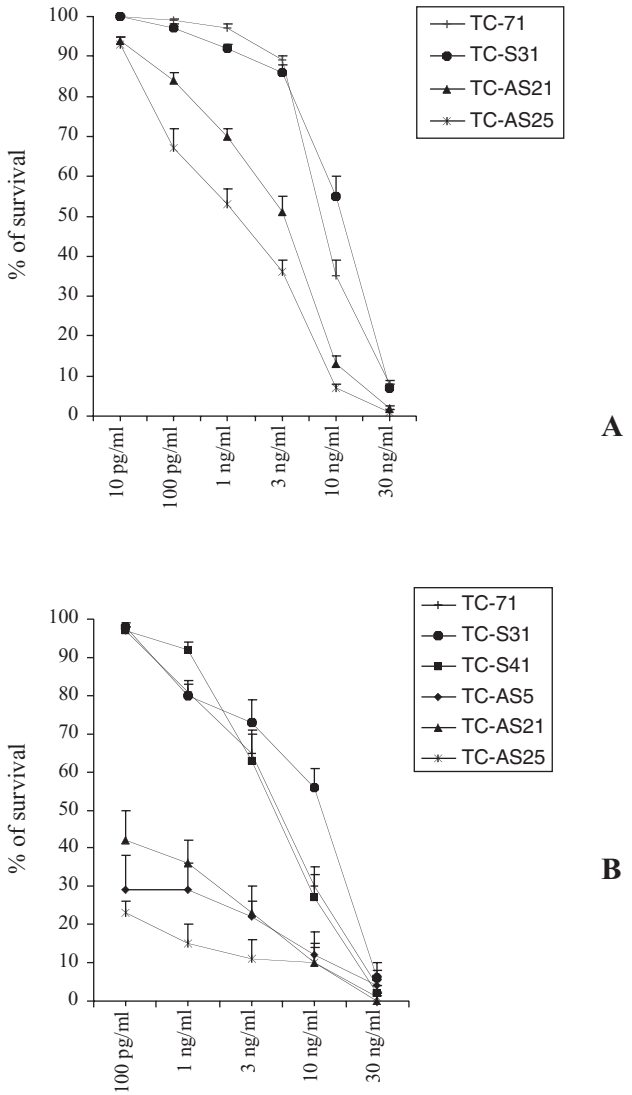

Figure 11 Cytotoxicity of DXR on TC-71 cells and derived clones in monolayer **(A)** and soft agar conditions **(B)**. See Materials and methods for a complete description of the procedures used. Results represent the mean ± SE of triplicate experiments. TC/S, sense-transfected clones; TC/AS, antisense-transfected clones.

supporting the view of IGF-IR as an important factor in the regulation of apoptosis in mammalian cells.[33] The significant decrease of anchorage-independent growth in soft agar by TC/AS clones suggests that the malignant phenotype of ES cells has been reversed after treatment with antisense IGF-IR. These findings, together with the observed significant *in vitro* reduction of TC/AS motility, supported the possibility that IGF-IR impairing strategies may have an effective role also *in vivo*. Indeed, we demonstrated a significant delay in tumor formation and a reduction in the *in vivo* growth rate of TC/AS tumors. Moreover, colony formation, after i.v. injection of TC-71 cells, was significantly impaired. Lung colonies were never observed in mice injected with TC/AS cells. The formation of extrapulmonary colonies was significantly delayed, and their incidence and number were significantly lower in the two TC/AS clones examined. The *in vivo* inhibitory effects were particularly evident for the TCAS21 transfectant, in agreement with the lower *in vitro* mitogenic and anchorage-independent growth ability of this clone in comparison with the others. However, compared with the treatment effects of antisense plasmids stably transfected in other cell systems, the *in vivo* effectiveness of IGF-IR antisense strategies in ES cells is not striking. Several factors may be invoked in interpreting our findings. ES cells produce IGF-I and the antisense-transfected cells expressed residual levels of IGF-IR. It is therefore possible that, under conditions of high cell density, autocrine mechanism of stimulation was sufficient to rescue the subpopulation of cells expressing the required threshold level of IGF-IR, eventually giving rise to tumors. This is consistent with the observation that the latent period preceding the appearance of tumors is prolonged in TC/AS clones compared to controls. In addition, TC-71 cells show a higher malignant potential compared to other cell models in nude mice. If a more effective inhibition of receptor expression could be achieved (perhaps with more efficient vectors, or, alternatively, by the use of dominant negative constructs), the magnitude of the effect could be improved. Furthermore, the antitumor effects observed for antisense IGF-IR plasmids in syngeneic animal model systems are the result of a still poorly defined immunity induction besides the reduction of IGF-IR, which would not play a role in this human tumor xenograft model.

From a clinical point of view, to be of significant therapeutic value, targeted strategies need to be effectively combined with conventional chemotherapeutic drugs. Most anticancer agents, including DXR, kill cancer cells by inhibiting cell cycle and/or inducing apoptosis.[34,35] Apoptotic action of chemotherapeutic drugs has been extensively studied in the last few years, and has been claimed to be their main mechanism of action. On the other hand, IGF-IR, activated by its ligands, is emerging as a powerful inhibitor of apoptosis induced by a variety of agents, including anticancer drugs, and ionizing and nonionizing radiation.[36–39] In ES, a recent study clearly indicates that IGF-I can act as a survival factor and that activation of IGF-IR renders the cells more resistant to DXR-induced apoptosis.[27] Therefore, impairment of IGF-IR functions may sensitize ES cells to apoptosis induced by chemotherapeutic drugs, therefore potentiating their cytotoxic action. Indeed, we found that chemosensitivity against DXR, a major drug for the treatment of ES patients, is significantly higher in IGF-IR AS clones with respect to controls, confirming that the disruption of IGF-IR may potentiate the effects of chemotherapeutic agents.

Taken together, these findings indicate that the inhibition of IGF-IR by antisense strategies may be relevant to the clinical treatment of ES patients by increasing the possibility of curing these neoplasms with strategies aimed at IGF-IR inactivation. When combined with the development of viral vectors designed to deliver genetic information with high efficiency, these strategies could form the basis for the development of highly specific, antimetastatic therapies in patients with ES.

Acknowledgments

This work was supported by grants from the Italian Association for Cancer Research, the Italian Ministry for University and Research, and the Rizzoli Institute. VC is the recipient of a Fellowship from the Italian Foundation for Cancer Research. We thank Renato Baserga (Kimmel Cancer Center, Thomas Jefferson University) for kindly providing us with the plasmid expressing antisense sequences to IGF-IR RNA.

References

1. Delattre O, Zucman J, Melot T, et al. The Ewing family of tumors — a subgroup of small-round-cell tumors defined by specific chimeric transcripts. *N Engl J Med.* 1994;331:294–299.
2. Ambros IM, Ambros PF, Strehl S, Kovar H, Gadner H, Salzer Kuntschik M. MIC2 is a specific marker for Ewing's sarcoma and peripheral primitive neuroectodermal tumors. Evidence for a common histogenesis of Ewing's sarcoma and peripheral primitive neuroectodermal tumors from MIC2 expression and specific chromosome aberration. *Cancer.* 1991;67:1886–1893.
3. Kovar H, Dworzak M, Strehl S, et al. Overexpression of the pseudoautosomal gene MIC2 in Ewing's sarcoma and peripheral primitive neuroectodermal tumor. *Oncogene.* 1990;45:1067–1070.
4. Campanacci M. Bone and Soft Tissue Tumors, 2nd ed. Wien: Springer-Verlag, 1999.
5. Bacci G, Toni A, Avella M, et al. Long-term results in 144 localized Ewing's sarcoma patients treated with combined therapy. *Cancer.* 1988;63:1477–1486.
6. Burgert EO, Nesbit ME, Garnsey LA, et al. Multimodal therapy for the management of nonpelvic, localized Ewing's sarcoma of bone: intergroup study IESS-II. *J Clin Oncol.* 1990;8:1514–1524.
7. Paulussen M, Ahrens S, Craft AW, et al. Ewing's tumors with primary lung metastases: survival analysis of 114 (European Intergroup) cooperative Ewing's sarcoma studies patients. *J Clin Oncol.* 1998;16:3044–3052.
8. Bacci G, Picci P, Ferrari S, et al. Neoadjuvant chemotherapy for Ewing's sarcoma of bone. No benefit observed after adding iphosphamide and etoposide to vincristine, actinomycin, cyclophosphamide, and doxorubicin in the maintenance phase. Results of two sequential studies. *Cancer.* 1998;6:1174–1183.
9. Craft A, Cotterill S, Malcolm A, et al. Ifosfamide-containing chemotherapy in Ewing's sarcoma: the Second United Kingdom Children's Cancer Study Group and the Medical Research Council Ewing's Tumor Study. *J Clin Oncol.* 1998;16:3628–3633.
10. Yee D, Favoni RE, Lebovic GS, et al. Insulin-like growth factor I expression by tumors of neuroectodermal origin with the t(11;22) chromosomal translocation. A potential autocrine growth factor. *J Clin Invest.* 1990;86:1806–1814.
11. Scotlandi K, Benini S, Sarti M, et al. Insulin-like growth factor I receptor–mediated circuit in Ewing's sarcoma/peripheral neuroectodermal tumor: a possible therapeutic target. *Cancer Res.* 1996;56:4570–4574.
12. Toretsky JA, Kalebic T, Blakesley V, LeRoith D, Helman LJ. The insulin-like growth factor-I receptor is required for EWS/FLI-1 transformation of fibroblasts. *J Biol Chem.* 1997; 272:30822–30827.
13. Scotlandi K, Benini S, Nanni P, et al. Blockage of insulin-like growth factor-I receptor inhibits the growth of Ewing's sarcoma in athymic mice. *Cancer Res.* 1998;58:4127–4131.
14. Resnicoff M, Coppola D, Sell C, Rubin R, Ferrone S, Baserga R. Growth inhibition of human melanoma cells in nude mice by antisense strategies to the type 1 insulin-like growth factor receptor. *Cancer Res.* 1994;54:4848–4850.
15. Resnicoff M, Sell C, Rubini M, et al. Rat glioblastoma cells expressing an antisense RNA to the insulin-like growth factor-1 (IGF-1) receptors are nontumorigenic and induce regression of wild-type tumors. *Cancer Res.* 1994;54:2218–2222.
16. Heid CA, Stevens J, Livak KJ, Williams PM. Real time quantitative PCR. *Genome Res.* 1996;6:986–994.
17. Gibson UE, Heid CA, Williams PM. A novel method for real time quantitative RT-PCR. *Genome Res.* 1996;6:995–1001.
18. Bradford MM. A rapid and sensitive method for the quantitation of microgram quantities of proteins utilizing the principle of protein–dye binding. *Anal Biochem.* 1976;72:248–254.
19. Folkman J, Moscona A. Role of cell shape in growth control. *Nature.* 1978;273:345–349.
20. Valentinis B, Reiss K, Baserga R. Insulin-like growth factor-I–mediated survival from anoikis: role of cell aggregation and focal adhesion kinase. *J Cell Physiol.* 1998;176:648–657.
21. Valentinis B, Morrione A, Peruzzi F, Prisco M, Reiss K, Baserga R. Anti-apoptotic signaling of the IGF-I receptor in fibroblasts following loss of matrix adhesion. *Oncogene.* 1999;18:1827–1836.
22. Aaronson TA, Todaro GJ. Basis for the acquisition of malignant potential by mouse cells cultivated *in vitro*. *Science.* 1968;162:1024–1026.
23. Scotlandi K, Benini S, Manara MC, et al. Murine model for skeletal metastases of Ewing's sarcoma. *J Orthop Res.* 2000;18:959–966.
24. van Valen F, Winkelmann W, Jurgens H. Type I and type II insulin-like growth factor receptors and their function in human Ewing's sarcoma cells. *J Cancer Res Clin Oncol.* 1992;118:269–275.
25. De Alava E, Kawai A, Healey JH, et al. EWS–FLI1 fusion transcript structure is an independent determinant of prognosis in Ewing's sarcoma. *J Clin Oncol.* 1998;16:1248–1255.
26. De Alava E, Panizo A, Antonescu CR, et al. Association of EWS/FLI1 type 1 fusion with lower proliferative rate in Ewing's sarcoma. *Am J Pathol.* 2000;156:849–855.
27. Toretsky JA, Thakar M, Eskenazi AE, Frantz CN. Phosphoinositide 3-hydroxide kinase blockade enhances apoptosis in the Ewing's sarcoma family of tumors. *Cancer Res.* 1999; 59:5745–5750.
28. Long L, Rubin R, Baserga R, Brodt P. Loss of the metastatic phenotype in murine carcinoma cells expressing an antisense RNA to the insulin-like growth factor receptor. *Cancer Res.* 1995;55:1006–1009.
29. Lee C-T, Wu S, Gabrilovich D, et al. Antitumor effects of an adenovirus expressing antisense insulin-like growth factor I receptor on human lung cancer cell lines. *Cancer Res.* 1996;56:3038–3041.
30. Burfeind P, Chernicky CL, Rininsland F, Ilan J, Ilan J. Antisense RNA to the type I insulin-like growth factor receptor suppresses tumor growth and prevents invasion by rat prostate cancer cells *in vivo*. *Proc Natl Acad Sci USA.* 1996;93:7263–7268.
31. Nakamura K, Hongo A, Kodama J, Miyagi Y, Yoshinouchi M, Kudo T. Down-regulation of the insulin-like growth factor I receptor by antisense RNA can reverse the transformed phenotype of human cervical cancer cell lines. *Cancer Res.* 2000;60:760–765.
32. Chernicky CL, Yi L, Tan H, Gan SU, Ilan J. Treatment of

human breast cancer cells with antisense RNA to the type I insulin-like growth factor receptor inhibits cell growth, suppresses tumorigenesis, alters the metastatic potential, and prolongs survival *in vivo*. *Cancer Gene Ther.* 2000;7:384–395.
33. Baserga R, Hongo A, Rubini M, Prisco M, Valentinis B. The IGF-I receptor in cell growth, transformation and apoptosis. *Biochim Biophys Acta.* 1997;1332:F105–F126.
34. Eastman A. Activation of programmed cell death by anticancer agents: cisplatin as a model system. *Cancer Cells.* 1990;2:275–280.
35. Waldman T, Zhang Y, Dillehay L, et al. Cell-cycle arrest *versus* cell death in cancer therapy. *Nat Med.* 1997;3:1034–1036.
36. Sell C, Baserga R, Rubin R. Insulin-like growth factor I (IGF-I) and the IGF-I receptor prevent etoposide-induced apoptosis. *Cancer Res.* 1995;55:303–306.
37. Turner BC, Haffty BG, Narayanan L, et al. Insulin-like growth factor 1 receptor overexpression mediates cellular resistance and local breast cancer recurrence after lumpectomy and radiation. *Cancer Res.* 1997;57:3079–3083.
38. Nakamura S, Watanabe H, Miura M, Sasaki T. Effect of the insulin-like growth factor 1 receptor on ionizing radiation-induced cell death in mouse embryo fibroblast. *Exp Cell Res.* 1997;235:287–294.
39. Dunn SE, Hardman RA, Kari FW, Barrett CJ. Insulin-like growth factor 1 (IGF-I) alters drug sensitivity of HBL 100 human breast cancer cells by inhibition of apoptosis induced by diverse anticancer drugs. *Cancer Res.* 1997;57:2687–2693.